Time-minimal orbital transfers to temporarily-captured natural Earth satellites

Monique Chyba, Mikael Granvik,Robert Jedicke,Geoff Patterson,Gautier Picot, Jeremie Vaubaillon

Abstract In this paper we focus on time-optimal transfers from a geostationary orbit to a sample of Natural Earth Satellites (NES) for a spacecraft using low thrust propulsion. Based on prior work we first analyze rendezvous missions in a vicinity of the Earth-Moon $L1$ equilibrium point, using a range of low thrusts from 0.2N to 1.0N. As a first approach, we approximate the dynamics of the spacecraft subject to the gravitational field of the Earth and the Moon by the planar restricted three-body model, before considering the spatial restricted three-body model. The time optimal control strategies are calculated using classical indirect methods of optimal control based on the Pontryagin Maximum Principle. We verify the local optimality of the corresponding trajectories using second order conditions.

Monique Chyba
Department of Mathematics, University of Hawaii at Manoa, 2565 McCarthy Mall, Honolulu, Hawaii 96822 USA e-mail: mchyba@math.hawaii.edu

Mikael Granvik
Department of Physics, P.O. Box 64, 00014 University of Helsinki, Finland e-mail: mgranvik@iki.fi

Robert Jedicke
Institute for Astronomy, 2680 Woodlawn Drive, Honolulu, HI 96822-1839 USA e-mail: jedicke@ifa.hawaii.edu

Geoff Patterson
Department of Mathematics, University of Hawaii at Manoa, 2565 McCarthy Mall, Honolulu, Hawaii 96822 USA e-mail: geoff@math.hawaii.edu

Gautier Picot
Department of Mathematics, University of Hawaii at Manoa, 2565 McCarthy Mall, Honolulu, Hawaii 96822 USA e-mail: gautier@math.hawaii.edu

Jérémie Vaubaillon
Institut de Mécanique Céleste et de Calcul des Ephémérides, IMCCE, 77 Av. Denfert Rochereau, 75014 Paris FRANCE e-mail: vaubaill@imcce.fr

1 Introduction

In this paper, we present a first approach to the design of low-thrust time-minimal orbital transfers to temporarily-captured natural Earth satellites (NES). By definition a NES is a celestial body that orbits the Earth. More precisely, a natural object in space is defined as *temporarily-captured* by a planet (or any body orbiting the Sun, including the Moon) by requiring simultaneously, see [13], that

1. the planetocentric Keplerian energy $E_{planet} < 0$,
2. the planetocentric distance is less than three Hill radii for the planet in question (e.g., for the Earth $3R_{H,\oplus} \sim 0.03$ AU

In addition, for an object to be considered a temporarily-captured *orbiter* (TCO), we require that it makes at least one full revolution around the planet in a co-rotating frame while being captured (the line from the planet to the Sun is fixed in this coordinate system) [13]. As a convention for this paper, we will always be referring to TCO which orbit the Earth (though the definition is stated more generally), and so, in this paper, TCO will be equivalent to temporarily-captured NES.

Work described in Granvik et. al. (2012) [13] details a selection process of 10 million "test-particles" in space, whose trajectories are integrated in order to determine which qualify as TCO. Of the 10 million test-particles, they find that 18,096 become TCO. This characterization of the TCO population acts as a key precursor to our work. It is from this integrated TCO database of over eighteen-thousand meteoroids that we select our orbital transfer targets.

Statistically, it can be shown that at any given time there is at least one 1-m-diameter TCO orbiting the Earth [13]. There are several reasons why the TCO are appealing targets, in addition to the fact that transfers to TCO have otherwise been unexplored. Primarily, the fact that TCO are temporarily in orbit around Earth provides us with several luxuries: First, there is already much documentation regarding two of the primary bodies which act on the TCO near Earth– the Earth and the Moon. Second, an orbiting object allows more time for detection, planning, and execution of a space mission than an object which just flies by, (i.e. does not complete an orbit). Note that the average number of revolutions for a TCO is 2.88 ± 0.82 [13]. More reasons the TCO are attractive targets include their closeness to Earth, making for a more cost-effective and time-effective mission, than compared to a deep-space mission (e.g. the 7-year Hayabusa mission), and their small size, which introduces the possibility of returning with the entire TCO to Earth. A final reason that TCO make interesting targets is evident when examining figures of the trajectories of some of the TCO. While some follow what we will loosely define as *regular* orbits (i.e. elliptical, planar), others follow very *irregular* orbits (i.e. scattered, non-planar). This diversity of orbit trajectories is appealing (especially the irregular trajectories), since we can really test the limits of our transfer computation methods, and develop experience performing maneuvers that otherwise have not been completed.

In space navigation, we define an *orbital transfer* as the use of propulsion systems to change the orbit of a spacecraft from some initial orbit to a final orbit. Throughout

the paper "transfer" will always mean orbital transfer. The terms "engines" and "thrusters" will always refer to the propulsion system of our spacecraft.

For this work, we assume that our spacecraft starts on a geostationary orbit. The destination orbits for our transfers will be orbits of TCO. In this paper we identify *time-minimal* transfers, as opposed to optimizing other typical costs, such as fuel-consumption. We do this for several reasons: Computationally, this is a logical first step toward identifying fuel-efficient solutions in future work. Practically, the lifespans of TCO are typically short (286 ± 18 days) [13] which suggests time-minimization may be important in the actual development of a spacecraft mission. It is also worth noting that the time of capture would not necessarily be equal to the time of detection, meaning the lifespan of the TCO should be viewed as an upper bound on the amount of time available to complete a transfer. The detectability of TCOs is currently being studied.

The method used to find solutions in this work includes modeling the dynamics of our spacecraft using the restricted three-body problem. Indeed several TCO orbits are quite accurately approximated by trajectories of the well-known restricted 3-body problem [18] during an interval of time when they can be assumed to be evolving in the Earth-Moon system. Moreover, many of these TCO orbits pass through a small vicinity of the Lagrangian point L_1 where the gravitational fields of the Earth and the Moon compensate each other. Let us recall that the characteristics of the natural dynamics in the neighborhood of the Lagrangian points have already been investigated in depth to design low-energy space transfers, see for example [12, 15] Therefore, we chose to rendezvous with each TCO when the Euclidean distance from the L_1 to the TCO is at its smallest.

Our computations of time-minimal transfers toward orbits of TCO are based on indirect methods in optimal control. The optimal transfers are necessarily projections of extremal curves $(q(t), p(t))$ belonging to the cotangent bundle of the phase space. These extremal curves are solutions of the Hamiltonian system derived from the application of the Pontryagin Maximum Principle [17], and can be computed by means of a shooting method. This work relies on the two-dimensional high-thrust extremal trajectory from the geostationary orbit to the equilibrium point L_1 of the Earth-Moon system (described in [16]) as the reference transfer used to initialize the shooting method. More precisely, let the vector $q(t)$ represent the position and velocity of our spacecraft after time t. We set the initial condition q_0 on a geostationary orbit, and a terminal condition q_f. The task is to find the so-called initial adjoint vector p_0 and final time t_f, such that the projection of the corresponding extremal curve started from (q_0, p_0) and evaluated at t_f is the required terminal condition; i.e. $q(t_f) = q_f$. This can be achieved using a Newton method, provided that we are able to determine an initial guess for the value of p_0 which gives convergence of the algorithm. The algorithm is more robust to the initial guess for higher maximum thrust constraints. So, to obtain low-thrust transfers a continuation method is performed by using the maximum thrust allowed by the spacecraft engines as the homotopic parameter. The local optimality of the computed extremal is then verified using a second order condition, connected to the concept of conjugate points [1, 6, 8]. Such computations are done using the Matlab package Hampath [11].

To summarize, we provide collections of low-thrust orbital transfers from a geostationary orbit to a sample of orbits of TCO. More specifically, we compute two-dimensional and three-dimensional locally-time-optimal transfers using low propulsion for rendezvous with TCO in a small vicinity of the Earth-Moon Lagrangian point $L1$. In addition to providing the first numerical examples of space transfers to TCO, our computations expand on the work initiated in [4, 16] to apply fundamental tools from optimal control theory to design optimal three-dimensional space transfers towards non-Keplerian target orbits.

2 The Model

In this section, we describe the selection of TCO as target for our spacecraft mission, and we introduce the restricted 3-body problem to model the dynamics of our system.

2.1 Temporarily-Captured Orbiter

As stated in the introduction, our goal is to compute locally time-optimal transfers for a low-thrust spacecraft from the geostationary orbit to a sample of TCO. In this section we make explicit the motivation for our target selection for our transfers.

Figure 1 shows the orbits of six TCO from the Granvik et. al. database [13], which display a variety of orbit regularity. For this work, we approach transferring to a TCO by selecting a specific rendezvous point along that TCO's orbit as the destination for a transfer. By "rendezvous" we mean that the spacecraft must match the position and velocity of the TCO at the selected point.

The specific rendezvous point we select on a given TCO's orbit is based on results from [16]. In that paper, two-dimensional transfers using the restricted three-body model are completed to the Earth-Moon Lagrangian point $L1$. There is also evidence in [16] that the $L1$ point serves as a natural gateway to other transfer destinations, such as a parking orbit around the Moon. For these reasons we choose in this first approach to the problem to focus on rendezvous near the L_1 point.

Analysis of the TCO data shows that 12,586 TCO come within 1 Lunar Distance (LD) of the $L1$ point, and that 383 come within 0.1 LD of the $L1$ point. We choose to attempt our first transfers to a sample of 100 of these 383 TCO. One Lunar Distance (LD) is defined as 384,400 km, an approximate average distance between the Earth and the Moon. The particular point along each TCO trajectory we set as our destination is the point at which the Euclidean distance from the TCO to $L1$ is the smallest. Since the transfers in [16] were done in two-dimensions, the 100 selected TCO rendezvous points were those of the 383 closest which had the smallest absolute z-coordinates ($|z| \leq 0.0166$ LD, for all of the selected 100 TCO rendezvous).

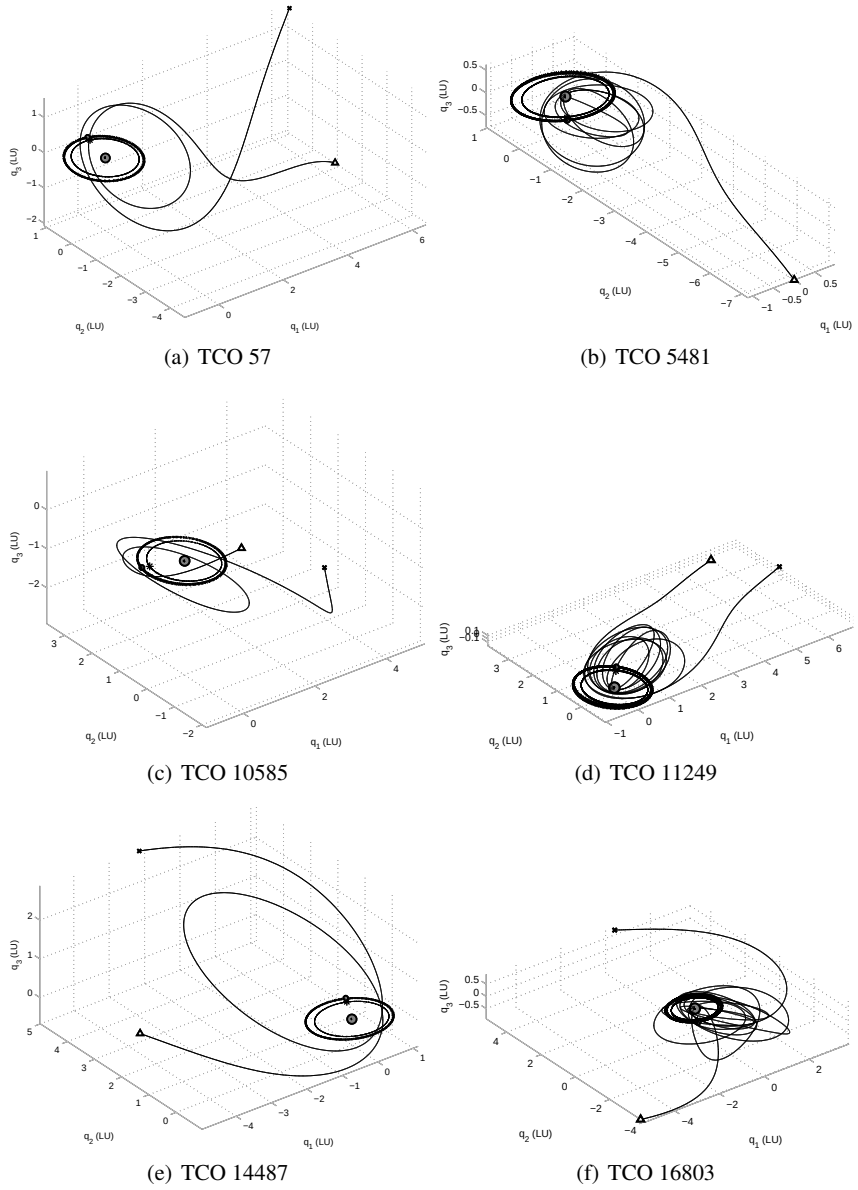

(a) TCO 57 (b) TCO 5481

(c) TCO 10585 (d) TCO 11249

(e) TCO 14487 (f) TCO 16803

Fig. 1 Example orbits of six distinct TCO with a variety of regularity, viewed in the inertial frame. The Earth is the large circle, and the orbits of the Moon and $L1$ point are the thick black outer and inner rings, respectively. The thin black curves are the paths of the TCO, from point of capture (marked as a triangle) to point of escape (marked as an X).

Table 1 display data for 21 TCO for which succesful transfers using the method described in this article have been computed.

TCO #	Filename	$d_E(q_{rend} - L1)$	t_{rend} (d)	T_{capt} (d)	n_{orbits}
57	'NESC000008fB'	0.0736	200.8	285.6	1.3805
651	'NESC00001QEL'	0.0644	32.9	115.8	-1.1862
2778	'NESC000072MS'	0.0249	118.8	147.7	1.5195
3813	'NESC00009lwe'	0.0540	133.3	214.4	1.4137
3867	'NESC00009paY'	0.0617	65.2	222.4	1.3699
3955	'NESC00009vo1'	0.0392	46.8	89.6	-1.1765
4227	'NESC0000aEqt'	0.0208	66.9	2824.8	52.4112
4980	'NESC0000csxH'	0.0400	78.8	377.6	-2.1725
5481	'NESC0000dpsc'	0.0613	326.7	373.4	5.1306
7548	'NESC0000iVXy'	0.0406	78.6	216.6	1.3947
7628	'NESC0000j7Zq'	0.0197	141.6	162.1	1.4688
8962	'NESC0000mCKB'	0.0802	84.2	401.0	5.0309
10585	'NESC0000qeLr'	0.0862	64.2	206.5	1.3799
10747	'NESC0000qScl'	0.0246	62.5	128.3	-1.2733
10979	'NESC0000rEjx'	0.0319	59.2	188.9	1.3092
11249	'NESC0000s1QJ'	0.0339	75.7	562.2	7.4318
12028	'NESC0000tzdR'	0.0235	438.4	454.0	-1.0241
13933	'NESC0000yPwy'	0.0980	25.2	478.4	-1.1105
14487	'NESC0000AIeg'	0.0145	131.9	185.5	1.3544
16519	'NESC0000EZv7'	0.0829	921.3	1217.9	12.4351
16803	'NESC0000Fpds'	0.0853	244.8	826.5	8.3719

Table 1 A table containing some data for each TCO that we completed a 0.2N transfer to (either two or three dimensional). Column 3 gives the Euclidean distance $d_E(q_{rend} - L1)$ in LD between q_{rend} and $L1$, and column 4 gives the time t_{rend} in days after initial capture that q_{rend} occurs. Column 5 displays the total amount of time T_{capt} in days that the TCO is captured, and column 6 gives the number of orbits n_{orbits} the TCO makes around the Earth.

Though we choose the rendezvous point to be near $L1$ to use knowledge derived from a previous study, an obvious extension for future work would be to select rendezvous points elsewhere on the TCO trajectories.

2.2 The circular restricted 3-body problem

The classical model used to approximate the motion of a spacecraft subject to the respective gravitational fields of the Earth and the Moon is the well-known restricted 3-body problem. The two main bodies, called *primaries* and denoted by their mass M_1 (Earth) and M_2 (Moon), are assumed to be a distance of one unit of length from each other and to have a total mass normalized to 1. They are revolving circularly around their center of mass G under the influence of their mutual gravitational attraction, with an angular velocity of 1. This assumption is reasonable as a first approximation to describe the Earth-Moon system since the eccentricity and incli-

nation of the Moon's orbit around the Earth are small (0.0549^o and 5.145^o to the ecliptic, respectively) The third body (the spacecraft), of negligible mass and denoted M, evolves in the 3-dimensional space without affecting the motion of the primaries. Let us note also that, in our problem, a TCO is assumed to be a point of negligible mass which we want the spacecraft to rendezvous with. Thus, our final conditions are that the spacecraft and the TCO share the exact same position and velocity at the final time of the transfer.

Let us denote $\mu = \frac{M_2}{M_1+M_2} \in [0, \frac{1}{2}]$ the reduced mass of the problem and use a dynamical coordinates system centered at G, rotating with an angular velocity 1 so that the primaries M_1 and M_2 are respectively located at the fixed locations $(-\mu,0,0)$ and $(1-\mu,0,0)$. The position of an object of negligible mass evolving in the Earth-Moon system at time t is denoted $(x(t),y(t),z(t))$. The equations of motion of the object derived from Newton's laws, are thus written [18]

$$\ddot{x} - 2\dot{y} = \frac{\partial V}{\partial x},\ \ddot{y} + 2\dot{x} = \frac{\partial V}{\partial y},\ \ddot{z} = \frac{\partial V}{\partial z} \tag{1}$$

where $-V$ is the mechanical potential defined by

$$V = \frac{x^2+y^2}{2} + \frac{1-\mu}{\rho_1} + \frac{\mu}{\rho_2} + \frac{\mu(1-\mu)}{2}. \tag{2}$$

with $\rho_1 = \sqrt{\left((x+\mu)^2+y^2+z^2\right)}$, $\rho_2 = \sqrt{\left((x-1+\mu)^2+y^2+z^2\right)}$ representing the distances from the spacecraft to the primaries. The Hamiltonian formalism [18] of the system is obtained by setting a new system of coordinates

$$v_1 = x,\ v_2 = y,\ v_3 = z,\ w_1 = \dot{x} - y,\ w_2 = \dot{y} + x,\ w_3 = \dot{z},$$

with the corresponding Hamiltonian function

$$H_0(v,w) = \frac{1}{2}(w_1^2 + w_2^2 + w_3^2) + w_1 v_2 - w_2 v_1 - \frac{1-\mu}{\rho_1} - \frac{\mu}{\rho_2} \tag{3}$$

being the only known first integral of the motion. In the Lagrangian formulation, equation (3) becomes

$$E(x,y,z,\dot{x},\dot{y},\dot{z}) = \frac{\dot{x}^2+\dot{y}^2+\dot{z}^2}{2} - V(x,y,z)$$

which is therefore constant along the solutions of the system (1). As a consequence the solutions of system (1) are constrained to be in the level sets given by

$$M(e) = \{(x,y,z,\dot{x},\dot{y},\dot{z}) \mid E(x,y,z,\dot{x},\dot{y},\dot{z}) = e\}$$

where the energy e is a real number. The *Hill's regions* are the projections of these level sets on the position space

$$H(e) = \{(x,y,z) \mid V(x,y,z) + e \geq 0\}.$$

System (1) has five equilibrium points defined as the critical points of the potential V. They are all located in the (x,y) plane and divided in two different types. The *Euler points*, denoted L_1, L_2 and L_3, located on the line $y = 0$ defined by the primaries, are non-stable, according to the Arnold's stability theorem [3]. The *Lagrange points* L_4 and L_5 each form an equilateral triangle with the two primaries. They are stable when μ satisfies the inequality $\mu < \mu_1 = \frac{1}{2}(1 - \frac{\sqrt{69}}{9})$ which is the case for the Earth-Moon system. See Figure 2 for an illustration of the equilibrium points

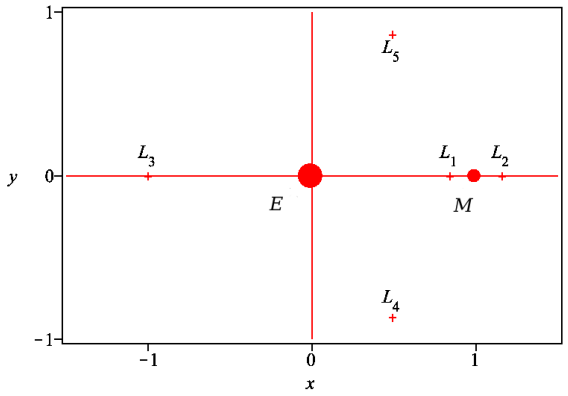

Fig. 2 The five equilibrium points of the Earth-Moon system, displayed in the rotating frame of the restricted three-body problem. The primaries E and M represent respectively the Earth and the Moon.

The topology of the Hill's region [18] depends on the energy e. The energy levels e_i corresponding to the critical points L_i satisfy $e_1 < e_2 < e_3 < e_4 = e_5$ and therefore define five phase portraits for the evolution of the object with respect to system (1) illustrated in figure 4.

This problem can be simplified by considering the *planar restricted 3-body problem* in which the motion is supposed to be restrained to the plane $\{z = 0\}$. This model is simply obtained by removing the z coordinate from the expression of the potential $-V$, which doesn't affect the critical levels involved in the modifications of the Hill's regions of energy, nor the locations of the equilibrium points.

The *controlled restricted 3-body problem* in the rotating frame, formulated by adding control terms representing the thrust of the spacecraft in the equation of the system (1), is simply written

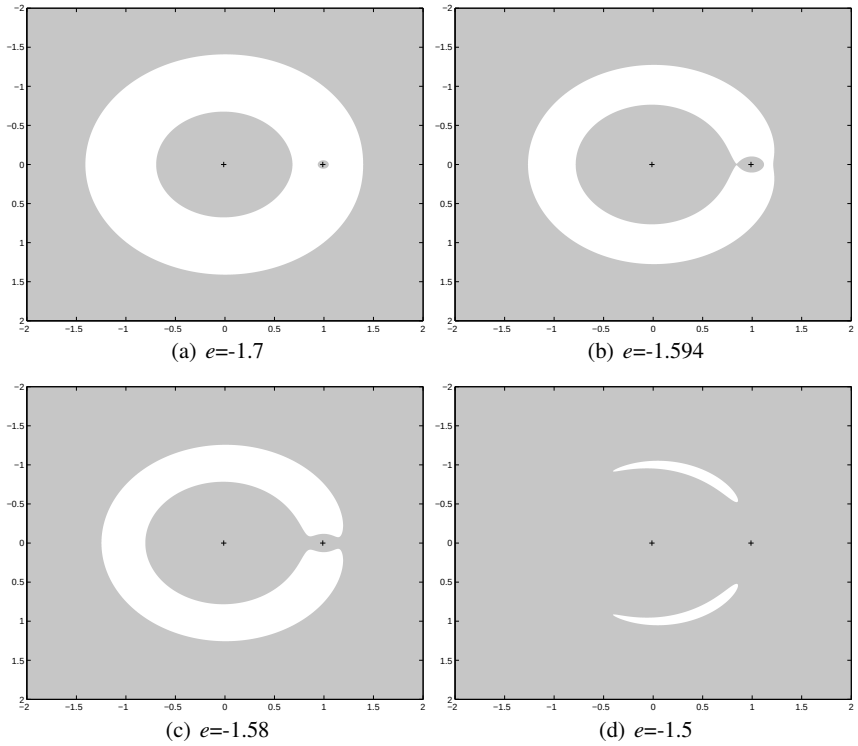

(a) e=-1.7 (b) e=-1.594

(c) e=-1.58 (d) e=-1.5

Fig. 3 Portraits of the Hill's regions with respect to e when μ =1.2153e-2 (Earth-Moon system). In every picture, the left and right black crosses respectively represent the Earth and the Moon. The regions of motion are displayed in gray.

$$\ddot{x}-2\dot{y}=\frac{\partial V}{\partial x}+u_1,\ \ddot{y}+2\dot{x}=\frac{\partial V}{\partial y}+u_2,\ \ddot{z}=\frac{\partial V}{\partial z}+u_3. \tag{4}$$

In this situation the Hamiltonian is given by

$$H(v,w)=H_0(v,w)-v_1u_1-v_2u_2-v_3u_3. \tag{5}$$

In this paper, we focus on minimizing the transfer time from the geostationary orbit to orbits of temporarily captured objects in the Earth-Moon system, when a low maximum thrust is allowed by the spacecraft's engines. The control $u=(u_1,u_2,u_3)$ represents then the impact of the engine on the spacecraft acceleration along every direction and the norm $\|u\|$ is the thrust. As a result, the mathematical formulation of our problem is to compute solutions of the system (4) which minimize the transfer time expressed as an integral cost by

$$\min_{u(\cdot)\in B_{\mathbb{R}^3}(0,\varepsilon)} \int_{t_0}^{t_f} 1 \, dt \tag{6}$$

where ε is the maximum thrust allowed by spacecraft's engines. Let us notice that, as for the Kepler problem, see [10], the spacecraft mass variation may be modelled dividing each component u_i, $i = 1,\ 2,\ 3$, by the spacecraft mass $m(t)$ at time t and considering the equation $\dot{m} = -\delta\|u\|$. This will not be taken into account in the work presented in this paper.

3 Indirect methods in optimal control

The indirect methods in optimal control provide numerical techniques to compute solutions of optimal control problems, based on geometric considerations. We briefly recall in this section their principle and the fundamental results they are derived from.

3.1 The Pontryagin Maximum Principle

Let M and U be two smooth manifolds of respective dimensions n and m and consider a general control system written

$$\begin{cases} \dot{q}(t) = f(q(t),u(t)) \\ \min_{u(.)} \int_0^{t_f} f^0(q(t),u(t))dt \\ q(0) = q_0 \in M_0,\ q(t_f) \in M_1 \end{cases} \tag{7}$$

where $f : M \times U \longrightarrow TM$ and $f^0 : M \times U \longrightarrow \mathbb{R}$ are smooth, $u(.)$ is a bounded measurable function defined on $[0,t(u)] \subset \mathbb{R}^+$ and valued in U, $t_f < t(u)$ and M_0 and M_1 are two subsets of M. A control $u(.)$ is said to be an *admissible control on* $[0,t_f]$ if its corresponding trajectory $q(.)$ satisfies $q_0 \in M_0$ and $q(t_f) \in M_1$. According to the Pontryagin Maximum Principle [17], for an admissible control $u(.)$ to be optimal, there exists a non-positive real p^0 and an absolutely continuous map $p(.)$ on $[0,t_f]$ called the *adjoint vector* such that $p(t) \in T^*_{q(t)}M$, $(p^0,p) \neq (0,0)$ and, almost everywhere on $[0,t_f]$, the following holds

$$\dot{q} = \frac{\partial H}{\partial p}(q,p,p^0,u), \quad \dot{p} = -\frac{\partial H}{\partial q}(q,p,p^0,u), \tag{8}$$

where H is the *pseudo-Hamiltonian* function

$$\begin{aligned} H : T^*M \times \mathbb{R}^*_- \times U &\longrightarrow \mathbb{R} \\ (q,p,p^0,u) &\longrightarrow p^0 f^0(q,u) + < p, f(q,u) > . \end{aligned}$$

The optimal control must also satisfy the maximization condition

$$H(q(t),p(t),p^0,u(t)) = \max_{v\in U} H(q(t),p(t),p^0,v) \tag{9}$$

almost everywhere on $[0,t_f]$. This condition implies in particular that H is identically zero if the final time t_f is not fixed. Finally, if M_0 (resp. M_1) is a regular submanifold of M, the transversality condition

$$p(0) \perp T_{q(0)}M_0 \quad (\text{resp.} \quad p(t_f) \perp T_{q(t_f)}M_1). \tag{10}$$

has to be satisfied. A solution (q,p,p^0,u) of equations (8) and (9) is called an *extremal*. In the following we focus on solutions with $p^0 \neq 0$ and we can therefore assume $p^0 = -1$. When the control domain U is assumed to be a smooth manifold, we can identify U locally to $\mathbb{R}^m$ and the maximization condition becomes $\frac{\partial H}{\partial u} = 0$. Assuming then that $\frac{\partial^2 H}{\partial u^2}$ is negative definite along the extremal, a straightforward application of the implicit function theorem shows that extremal controls are actually smooth feedback functions of the state and adjoint vectors in a neighborhood of $u(.)$: $u_r(t) = u_r(q(t),p(t))$. The pseudo-Hamiltonian H can thus be written as a real Hamiltonian function $H_r(q,p) = H(q,p,u_r(q,p))$ and any extremal trajectory can be expressed as a solution $z = (q,p)$ of the Hamiltonian system

$$\begin{cases} \dot{z} = \overrightarrow{H_r}(z(t)) \\ z_0 = (q_0,p_0) \end{cases} \tag{11}$$

where $\overrightarrow{H_r} = (\frac{\partial H_r}{\partial p}, -\frac{\partial H_r}{\partial q})$ is the Hamiltonian vector field associated with H_r and $p_0 = p(0)$. Let us mention that, in the presented work, the control domains considered are the closed balls of $\mathbb{R}^2$ and $\mathbb{R}^3$ with radius ε, which are not manifolds. However, in both cases, extremal controls turn out to belong to the sphere of radius ε almost everywhere on $[0,t_f]$ and can still be written, almost everywhere, as feedback functions of the state and adjoint vectors, leading to the formulation of a real Hamiltonian function H_r, see sections 4.1 and 5.1 for details.

3.2 Shooting function

The goal of the indirect method is to determine numerically extremals that satisfy the boundary conditions $q(0) = q_0 \in M_0,\ q(t_f) \in M_1$ and the transversality conditions. The difficulty is to determine the initial value of the adjoint vector p_0 such that the corresponding solution of (11) meets the conditions. We rewrite the boundary and transversality conditions under the form $R(z(0),z(t_f)) = \mathbf{0}$. Admissible extremals are now solutions of

$$\begin{cases} \dot{z} = \overrightarrow{H_r}(z(t)) \\ R(z(0),z(t_f)) = \mathbf{0}. \end{cases} \tag{12}$$

When the transfer time t_f is free, as in the time optimal case, solving the boundary value problem is then equivalent to solve the *shooting equation*. More precisely, this entails to find a zero of the so-called *shooting function* [7] S defined by

$$S : (p_0, t_f) \longrightarrow R(z_0, z_{t_f}). \tag{13}$$

In the free final time situation, the condition $H_r = 0$ is added to the function R. Notice that by construction S is a smooth function, and we can use a Newton type method to determine its zeroes.

3.3 Smooth continuation method

Newton methods are known to be very sensitive to an initial guess. The *smooth continuation method* [2, 19] is an efficient way to overcome this difficulty. The idea is to connect the Hamiltonian H_r to an Hamiltonian H_0, whose corresponding shooting equation is easy to solve, via a parametrized family $(H_\lambda)_{\lambda\in[0,1]}$ of smooth Hamiltonians. The algorithm is then divided into the following steps:

1. Solve the shooting equation associated with H_0;
2. Set up a discretization 0=λ_0, λ_1,..., λ_N=1 and solve iteratively the shooting equation associated with $H_{\lambda_{i+1}}$ by using as initial guess the solution of the shooting equation corresponding to H_{λ_i}.
3. The solution of the last shooting equation associated with H_{λ_N} is then a zero of the shooting function S.

3.4 Second order condition

The notion of conjugate points [6] plays a major role in our work for two reasons. First, the notion of conjugate points is at the origin of the so-called *second order optimality condition* which is a sufficient condition for an extremal to be locally optimal. Second, the non existence of a conjugate point along the solution of the continuation method for each λ_i guarantees the convergence of the algorithm, see [9, 14]. More precisely, focusing on the case $p^0 = -1$, to the Hamiltonian system (11) we associate the *Jacobi equation* equation on $T(T^*M)$

$$\dot{\delta}z(t) = d\overrightarrow{H}(z) \cdot \delta z(t) \tag{14}$$

along an extremal $z(.)$. A *Jacobi field* is a nontrivial solution $J(t) = (\delta q(t), \delta p(t))$ of the Jacobi equation along $z(.)$. A Jacobi field is said to be ***vertical*** at time t if $\delta q(t) = 0$. A time t_c is said to be a *geometrically conjugate time* if there exists a Jacobi field that is vertical at 0 and at t_c. In such a case, $q(t_c)$ is said to be *conjugate* to $q(0)$.

Conjugate times can be geometrically characterized by considering the *exponential mapping* defined, when the final time is assumed to be free, by

$$\exp_{q_0,t} : p_0 \longrightarrow q(t,q_0,p_0) \tag{15}$$

where $q(t,q_0,p_0)$ is the projection on the phase space of the solution $z(.)$ of (11) satisfying $z(0) = (q(0),p(0))$ and evaluated at the time t. Let us denote $\exp_t(\overrightarrow{H_r})$ the flow of $\overrightarrow{H_r}$. The following proposition results from a geometrical interpretation of the Jacobi equation [6].

Theorem 1. *Let $q_0 \in M$, $L_0 = T^*_{q_0}M$ and $L_t = \exp_t(\overrightarrow{H})(L_0)$. Then L_t is a Lagrangian submanifold of T^*M whose tangent space is spanned by Jacobi fields starting from L_0. Moreover $q(t_c)$ is geometrically conjugate to q_0 if and only if $\exp_{q_0,t_c}$ is not an immersion at p_0.*

Under generic assumptions, the following theorem connects the notion of conjugate time and the local optimality of extremals, see [1, 6, 8].

Theorem 2. *Let t_c^1 be the first conjugate time along z. The trajectory $q(.)$ is locally optimal on $[0,t_c^1)$ in C^0 topology. If $t > t_c^1$ then $q(.)$ is not locally optimal on $[0,t]$ in L^∞ topology.*

3.5 Hampath

The software Hampath, see [11], is designed along the indirect method described above. It also checks the second order optimality condition when smooth optimal control problems are considered. In particular, this package allows one to use shooting methods by initializing the shooting function by using a differential path-following method, and to compute the Jacobi of the Hamiltonian system to evaluate the conjugate times along an extremal solution.

4 Two-dimensional transfers

Our goal is to design three dimensional transfers to our sample pool of TCO. Toward this goal, developing two dimensional transfer will prove to be critical for the initialization of our methods.

4.1 Methodology

We focus on two-dimensional transfers by modeling the Earth-Moon system using the planar restricted three-body problem where the motion is restricted to the plane

$\{z=0\}$. Our motivation is to use existing planar time-optimal transfer to the L_1 point of the Earth-Moon system computed in ([16]). We compute transfers to planar projections of TCO passing in a neighborhood of the L_1 point.

The planar restricted three-body problem, with $q=(x,y,\dot{x},\dot{y})$ is given by the following bi-input system

$$\dot{q}=F_0(q)+F_1(q)u_1+F_2(q)u_2 \tag{16}$$

where

$$F_0(q)=\begin{pmatrix} q_3 \\ q_4 \\ 2q_4+q_1-(1-\mu)\frac{q_1+\mu}{((q_1+\mu)^2+q_2^2)^{\frac{3}{2}}}-\mu\frac{q_1-1+\mu}{((q_1-1+\mu)^2+q_2^2)^{\frac{3}{2}}} \\ -2q_3+q_2-(1-\mu)\frac{q_2}{((q_1+\mu)^2+q_2^2)^{\frac{3}{2}}}-\mu\frac{q_2}{((q_1-1+\mu)^2+q_2^2)^{\frac{3}{2}}} \end{pmatrix}$$

$$F_1(q)=\begin{pmatrix}0\\0\\1\\0\end{pmatrix},\ F_2(q)=\begin{pmatrix}0\\0\\0\\1\end{pmatrix},$$

Our objective is to compute low-thrust time-minimal numerical transfers from the geostationary orbit $\mathscr{O}_g$ to rendezvous with TCO at specific points on their orbits. In mathematical terms, our aim is to solve optimal control problems of the form

$$\begin{cases} \dot{q}=F_0(q)+F_1(q)u_1+F_2(q)u_2 \\ \min_{u(\cdot)\in B_{\mathbb{R}^2}(0,\varepsilon)}\int_{t_0}^{t_f}dt \\ q(0)\in\mathscr{O}_g,\ q(t_f)=q_{rend} \end{cases} \tag{17}$$

where ε is the maximum thrust, q_{rend} is the rendezvous point (i.e. q_{rend} is the position and velocity corresponding to the projection on the (x,y)-plane of a given TCO when it is nearest the point L_1) and t_f is the transfer time that we want to minimize. Applying the Pontryagin Maximum Principle in the normal case $p^0\neq 0$, it comes that every solution $q(t)$ of the optimal control problem (17) is necessarily the projection of an extremal curve $(q(t),p(t))$ solution of the system

$$\dot{q}(t)=\frac{\partial H}{\partial p},\ \dot{p}(t)=-\frac{\partial H}{\partial q} \tag{18}$$

where the pseudo-Hamiltonian function H is defined by

$$H(q,p,u)=-1+H_0(p,q)+\varepsilon(u_1H_1(p,q))+u_2H_2(p,q))$$

with $H_i(p,q)=\langle p,F_i(q)\rangle, i=0,\ 1,\ 2$ Moreover, we deduce from the maximization condition that, whenever $(H_1,H_2)\neq(0,0)$, the control u is given by

$$u_i = \frac{H_i}{\sqrt{H_1^2 + H_2^2}},\ i = 1,\ 2.$$

Substituting in H, yields the expression of the real Hamiltonian function

$$H_r(z) = -1 + H_0(z) + \varepsilon((H_1^2(z) + H_2^2(z))^{\frac{1}{2}})$$

which is identically zero on $[0, t_f]$ since the transfer time is not fixed. Defining the switching surface $\Sigma = \{H_1(p,q) = H_2(p,q) = 0\}$, an element $(q,p) \in \mathbb{R}^8 \backslash \Sigma$ is said to be of order 0. According to [5], every normal time-minimal extremal trajectory is a concatenation of a finite number of arcs of order 0 such that the control $u(.)$ instantaneously rotates by an angle π at junction points. More details about the structure of the extremals can be found in [5], we here focus on the practical application of the theory. Therefore, to compute time-minimal extremal trajectories we must find a zero the shooting equation

$$\begin{aligned} E : \mathbb{R}^5 &\longrightarrow \mathbb{R}^5 \\ (p_0, t_f) &\longrightarrow \begin{pmatrix} q(t_f) - q_{rend} \\ H_r(q(t_f), p(t_f)) \end{pmatrix}. \end{aligned}$$

We set q_0=(0.0947, 0, 0, 2.8792), expressed in the distance and time units of the restricted 3-body problem, as the initial point on the geostationary orbit. The mass of the spacecraft is assumed constant to 350 kg to compute the actual thrust value acting on the spacecraft. As stated in section 2.1 among a database of 18,096 TCO numerically simulated spatial trajectories we examined the 100 of those which come within 0.1 LD of $L1$ with the smallest absolute perpendicular coordinate to the plane defined by the motion of the Moon around the Earth, at the time they are nearest L_1. This choice was made, as a first approach, to guarantee that the dynamics of the considered trajectories with respect to this coordinate could be neglected so that they could be approximated by their two-dimensional projection on the plane of motion of the Moon for a significant interval of time. For reference, the largest absolute z-coordinate of any of the 100 selected TCO is $|z| = 0.0166$ LD. The projections on this plane have been calculated at every time by taking into account the position of the Moon in its orbit and the inclination of this orbit. The resulting two-dimensional trajectories have then been expressed as trajectories in the planar restricted 3-body problem by using the usual change of variable from the inertial to the rotating frame.

To provide a good initial guess for the shooting method to converge, we use a continuation method on the maximum control bound ε. Indeed, the higher the maximum control bound, the shorter the corresponding transfer time and the Newton algorithm converges easily to a solution of the shooting method. Therefore, by using the planar time-minimal transfer from the geostationary orbit to L_1 computed in [16] as an initial guess to initialize the shooting method, we first compute a reference extremal to each of the 100 selected TCO, associated with a maximum thrust of 1N, whose projection on the phase space is a candidate to be a time-minimal transfer. A discrete homotopic method on the parameter ε, is then used to determine

solutions of the shooting function for smaller control bound and thus candidates to be low-thrust time-minimal transfers from the geostationary to q_{rend}. At each step of the continuation algorithm, the first conjugate time along every generated extremal is computed to ensure, according to the second order condition, that it was locally time-optimal. All our computations are carried out using the software Hampath [11].

4.2 Results

Applying the methodology described in 4.1 for each of the selected 100 TCO, we get a collection of two-dimensional extremal transfers with thrusts from 1N to 0.2N. Note that a thrust of 1N is high enough to get good convergence of the shooting method, and a thrust of 0.2N was arbitrarily chosen as an acceptable low thrust value to rendezvous with the TCO.

Using the two-dimensional 1N $L1$ initialization from [16], we obtain 23 successful two-dimensional 1N TCO transfers. Using a continuation method from these 23 successes, we obtain 15 successful two-dimensional 0.2N TCO transfers. Data regarding the 15 transfers can be found on Table 2.

TCO #	t_f^1 (d)	t_c^1 (d)	$t_{rend} - t_f^1$	$t_f^{0.2}$	$t_c^{0.2}$	$t_{rend} - t_f^{0.2}$
57	11.1	12.5	189.7	47.2	49.8	153.6
651	19.4	∞	13.5	73.0	∞	-40.1
3813	10.1	14.0	123.2	56.0	∞	77.3
3867	10.2	16.6	55.0	55.1	61.8	10.2
4980	11.4	∞	67.4	58.0	62.3	20.9
5481	11.0	26.0	315.7	59.4	101.2	267.2
7548	12.2	17.7	66.5	59.3	420.4	19.3
8962	11.8	∞	72.4	60.0	76.9	24.2
10585	10.1	30.8	54.1	55.6	121.0	8.5
10979	10.1	∞	49.1	59.0	∞	0.3
11249	10.0	13.9	65.7	58.3	∞	17.5
12028	13.4	22.7	425.0	61.5	149.2	376.9
13933	10.7	14.1	14.4	59.4	65.1	-34.3
14487	10.1	22.6	121.8	58.5	∞	73.4
16803	10.7	15.0	234.1	66.5	91.8	178.3

Table 2 Data for the successful two-dimensional transfers. Column 2 gives the transfer times for the 1N transfers t_f^1, and column 3 gives the corresponding conjugate times t_c^1. Similarly, column 5 gives the transfer times for the 0.2N transfers $t_f^{0.2}$, and column 6 gives the corresponding conjugate times $t_c^{0.2}$. Note that a conjugate time marked ∞ means that no conjugate times were found within 100 times the transfer time. Columns 4 and 7 give the differences between the TCO rendezvous time and the transfer times. Note that a negative value in these columns means the transfer would be impractical, since we'd have to start the transfer before the TCO was captured (and therefore, likely before it was detected).

The durations of the successful two-dimensional 1N TCO transfers are all between 10.0106 days and 19.3920 days while the durations of the successful two-dimensional 0.2N TCO transfers are all between 47.2394 days and 72.9984 days. For 13 of the 15 low-thrust transfers, the transfer time $t_f^{0.2}$ is less than the time it takes the corresponding TCO to evolve from its time of capture to the rendezvous point. This remark is crucial from a practical stand point since it suggests that it may be feasible to detect a TCO enough in advance to launch a low-thrust time-optimal rendezvous mission.

Figure 4 gives examples of successful two-dimensional transfers using thrusts of 1N and 0.2N.

5 Three-dimensional transfers

In this section, we use results of section 4 to design three dimensional transfers.

5.1 Methodology

To compute three-dimensional time-minimal transfers to TCO, the methodology presented in 4.1 has to be adapted to take into account the vertical coordinate z. Let $q = (x, y, z, \dot{x}, \dot{y}, \dot{z})$, the controlled equations (4) are then expressed as the bi-input system

$$\dot{q} = F_0(q) + F_1(q)u_1 + F_2(q)u_2 + F_3(q)u_3 \tag{19}$$

where

$$F_0(q) = \begin{pmatrix} q_4 \\ q_5 \\ q_6 \\ 2q_5 + q_1 - (1-\mu)\frac{q_1+\mu}{((q_1+\mu)^2+q_2^2+q_3^2)^{\frac{3}{2}}} - \mu\frac{q_1-1+\mu}{((q_1-1+\mu)^2+q_2^2+q_3^2)^{\frac{3}{2}}} \\ -2q_4 + q_2 - (1-\mu)\frac{q_2}{((q_1+\mu)^2+q_2^2+q_3^2)^{\frac{3}{2}}} - \mu\frac{q_2}{((q_1-1+\mu)^2+q_2^2+q_3^2)^{\frac{3}{2}}} \\ -(1-\mu)\frac{q_3}{((q_1+\mu)^2+q_2^2+q_3^2)^{\frac{3}{2}}} - \mu\frac{q_3}{((q_1-1+\mu)^2+q_2^2+q_3^2)^{\frac{3}{2}}} \end{pmatrix}$$

$$F_1(q) = \begin{pmatrix} 0 \\ 0 \\ 0 \\ 1 \\ 0 \\ 0 \end{pmatrix}, \; F_2(q) = \begin{pmatrix} 0 \\ 0 \\ 0 \\ 0 \\ 1 \\ 0 \end{pmatrix}, \; F_3(q) = \begin{pmatrix} 0 \\ 0 \\ 0 \\ 0 \\ 0 \\ 1 \end{pmatrix}.$$

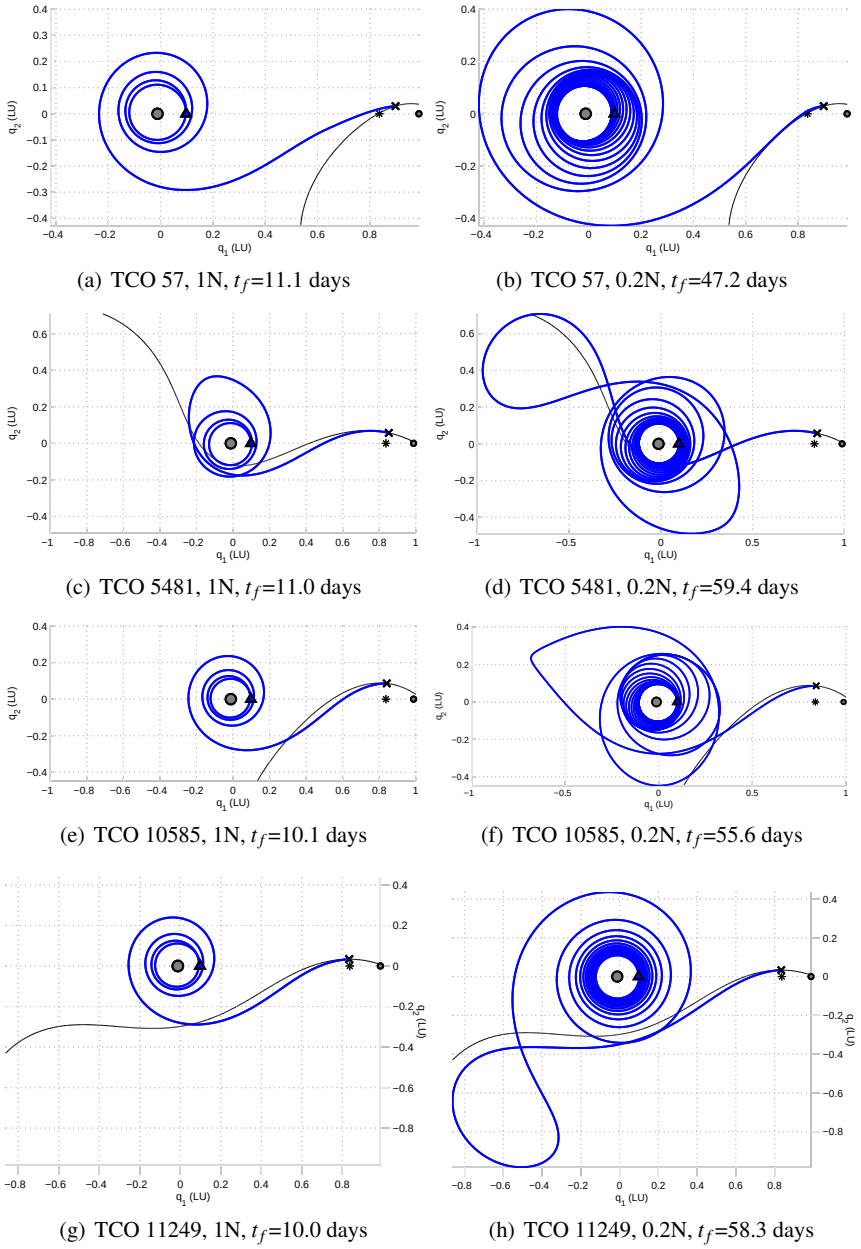

(a) TCO 57, 1N, t_f=11.1 days

(b) TCO 57, 0.2N, t_f=47.2 days

(c) TCO 5481, 1N, t_f=11.0 days

(d) TCO 5481, 0.2N, t_f=59.4 days

(e) TCO 10585, 1N, t_f=10.1 days

(f) TCO 10585, 0.2N, t_f=55.6 days

(g) TCO 11249, 1N, t_f=10.0 days

(h) TCO 11249, 0.2N, t_f=58.3 days

Fig. 4 Locally time-minimal two-dimensional transfers to four distinct TCO, associated with different thrusts, in the rotating frame. In each figure, the Earth (left) and the Moon (right) are shown as circles and the point L_1 by an asterisk. The thin black curves represent portions of the TCO trajectories. The thick blue curves represent the extremal transfer from the geostationary orbit (marked as a triangle) to the TCO (marked as an X).

and the optimal control problem that we have to solve in order to compute time-minimal numerical transfers between the geostationary orbit and a given TCO is written

$$\begin{cases} \dot{q} = F_0(q) + F_1(q)u_1 + F_2(q)u_2 + F_3(q)u_3 \\ \min_{u(\cdot)\in B_{\mathbb{R}^3}(0,\varepsilon)} \int_{t_0}^{t_f} dt \\ q(0) \in \mathscr{O}_g,\ q(t_f) = q_{rend} \end{cases} \tag{20}$$

Applying the Pontryagin Maximum Principle gives similar results to those obtained in the the two-dimensional problem. In the normal case $p^0 \neq 0$, every solution $q(t)$ of (20) is the projection of an extremal curve $(q(t), p(t))$ solution of the Hamiltonian system

$$\dot{q}(t) = \frac{\partial H_r}{\partial p},\ \dot{p}(t) = -\frac{\partial H_r}{\partial q} \tag{21}$$

where the Hamiltonian function H_r is given by

$$H_r(z) = -1 + H_0(z) + \varepsilon((H_1^2(z) + H_2^2(z) + H_3^2(z))^{\frac{1}{2}})$$

with $H_i(p,q) = \langle p, F_i(q)\rangle, i = 0,\ldots,3$. As in the two-dimensional problem, H_r is identically zero on $[0,t_f]$, the final time being free. Consequently, computing three-dimensional time-minimal extremal trajectories is performed by solving the shooting equation associated with the function

$$\begin{aligned} S : \mathbb{R}^7 &\longrightarrow \mathbb{R}^7 \\ (p_0, t_f) &\longrightarrow \begin{pmatrix} q(t_f) - q_{rend} \\ H_r(q(t_f), p(t_f)) \end{pmatrix}. \end{aligned}$$

We set the initial condition on the geostationary orbit as $q_0 = (0.0947, 0, 0, 0, 2.8792, 0)$, the mass of the spacecraft being assumed constant to 350 kg. The target set of TCO to reach is the same as in the two-dimensional problem, it is formed of the 100 TCO coming within 0.1 Lunar units of the point L_1 with the smallest absolute vertical coordinate z. There are two reasons for selecting these TCO. First, as in the two-dimensional problem, the circular restricted three-body problem provides a good approximation of their orbits in the close neighborhood of the L_1. In addition, the two-dimensional time-optimal transfers previously computed on the plane of motion of the Moon can be used to find initial guesses for the shooting method to converge.

In order to compute as many three-dimensional time-optimal transfers as possible, within a range of thrust from 0.2N to 1N, we propose two different approaches for the initialization of the shooting method. They are detailed below.

1. The first approach consists of using the two-dimensional transfer to L_1 associated with a thrust of 1N computed in ([16]) as an initial guess to directly compute three-dimensional transfers to TCO, associated with a thrust of 1N as well.

A continuation method on the control bound is then applied to compute three-dimensional transfers to TCO corresponding to lower thrusts.
2. The second way consists of using, for every TCO, the two-dimensional transfer associated with a thrust of 1N computed in section 4.1 as an initialization to compute a three-dimensional transfer associated with a thrust of 1N. A continuation on the control bound is then performed to compute three-dimensional transfers corresponding lower thrusts.

An important remark is that, as a convention, to initialize any three-dimensional transfer with an initialization from a two-dimensional transfer, we set the entries corresponding to the z coordinates equal to zero. Moreover, as in the two-dimensional problem, we used the second order condition to guarantee both the convergence of the continuation method and the local optimality of the computed transfers.

5.2 Results

Using the methodology described above, we have obtained the following results

- From the 15 two-dimensional 0.2N TCO transfer initializations, we obtain 5 successful three-dimensional 0.2N TCO transfers;
- From the 23 two-dimensional 1N TCO transfer initializations, we obtain 17 successful three-dimensional 1N TCO transfers. Using a continuation method, we obtain 13 successful three-dimensional 0.2N TCO transfers;
- From the two-dimensional 1N L1 initialization, we obtain 15 successful three-dimensional 1N TCO transfers. Using a continuation method, we obtain 12 successful three-dimensional 0.2N TCO transfers.

Note that some successes of one initialization strategy overlap with successes of other initialization strategies. In total we have 23 distinct successful three-dimensional 1N TCO transfers and 16 distinct successful three-dimensional 0.2N TCO transfers. The durations of the successful three-dimensional 1N TCO transfers are all between 10.0107 days and 19.4615 days while for the 0.2N transfers they are all between 55.3125 days and 81.4559 days. Table 3 displays data regarding the transfers.

Figure 5 gives examples of successful two-dimensional transfers using thrusts of 1N and 0.2N.

6 Conclusion and Future Work

This preliminary study provides the first numerical two-dimensional and three-dimensional time-optimal transfers to TCO. However, some limitations of the methods presented in this work prevent us from computing larger collections of such

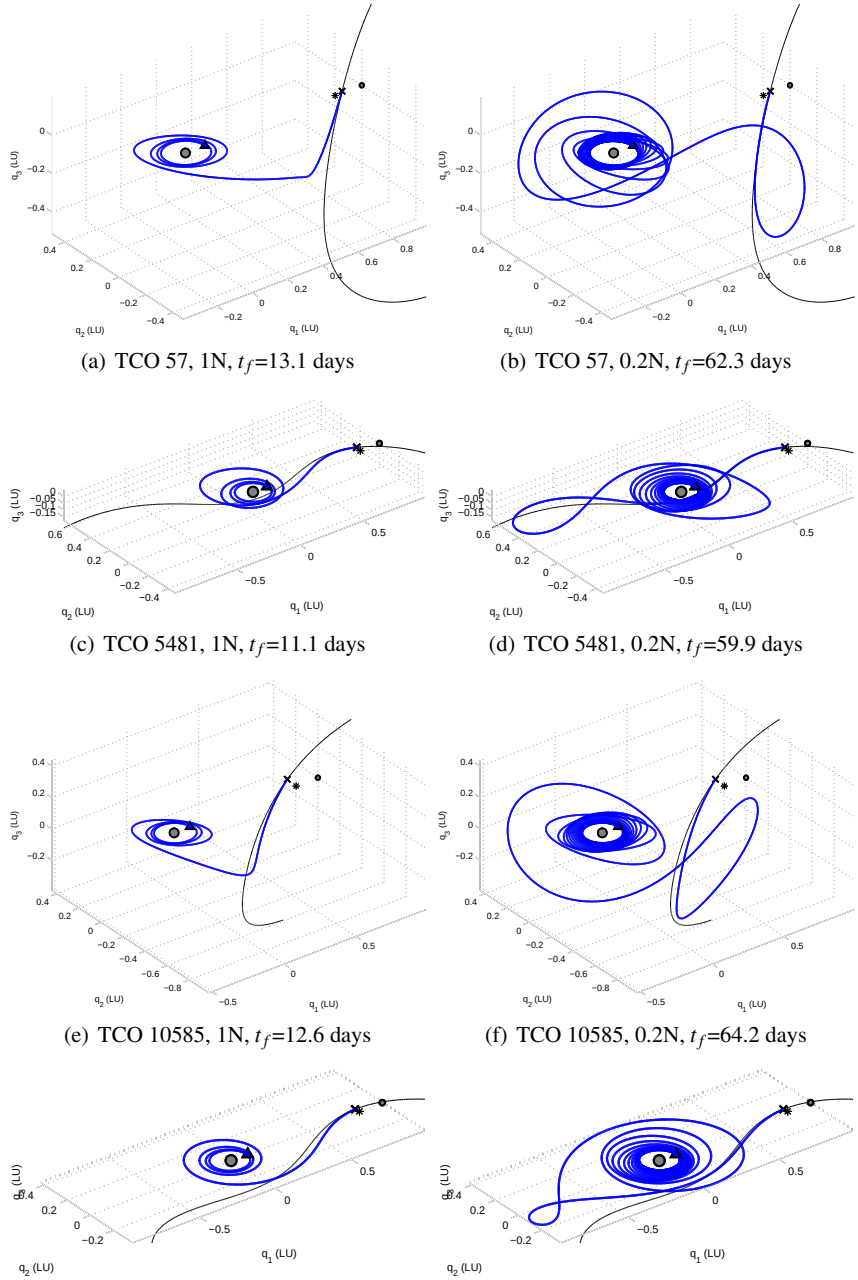

(a) TCO 57, 1N, t_f=13.1 days

(b) TCO 57, 0.2N, t_f=62.3 days

(c) TCO 5481, 1N, t_f=11.1 days

(d) TCO 5481, 0.2N, t_f=59.9 days

(e) TCO 10585, 1N, t_f=12.6 days

(f) TCO 10585, 0.2N, t_f=64.2 days

(g) TCO 11249, 1N, t_f=10.0 days

(h) TCO 11249, 0.2N, t_f=57.3 days

Fig. 5 Locally time-minimal three-dimensional transfers to four distinct TCO, associated with different thrusts, in the rotating frame. In each figure, the Earth (left) and the Moon (right) are shown as circles and the point L_1 by an asterisk. The thin black curves represent projections of portions of the TCO trajectories. The thick blue curves represent the extremal transfer from the geostationary orbit (marked as a triangle) to the TCO (marked as an X).

TCO #	t_f^1 (d)	t_c^1 (d)	$t_{rend} - t_f^1$	$t_f^{0.2}$	$t_c^{0.2}$	$t_{rend} - t_f^{0.2}$
57	13.1	15.6	187.6	62.3	67.3	138.5
651	19.5	28.4	13.4	81.5	91.2	-48.6
2778	18.6	20.2	100.2	77.7	80.1	41.1
3813	13.5	21.4	119.8	62.0	69.5	71.3
3955	19.3	26.9	27.5	80.6	89.4	-33.8
4227	10.1	68.4	56.8	55.3	∞	11.6
5481	11.1	13.2	315.6	59.9	107.0	266.8
7628	18.5	20.5	123.1	76.2	79.0	65.3
8962	11.9	19.2	72.4	65.1	82.8	19.1
10585	12.6	16.9	51.5	64.2	67.8	-0.1
10747	19.2	23.9	43.3	81.4	87.4	-18.8
10979	12.8	15.5	46.4	73.5	78.6	-14.3
11249	10.0	19.6	65.7	57.3	63.1	18.4
14487	12.8	16.5	119.1	62.9	66.8	69.0
16519	15.8	18.3	905.5	78.8	83.2	842.4
16803	10.8	14.6	234.0	67.1	70.7	177.7

Table 3 Data for the successful three-dimensional transfers. Column 2 gives the transfer times for the 1N transfers t_f^1, and column 3 gives the corresponding conjugate times t_c^1. Similarly, column 5 gives the transfer times for the 0.2N transfers $t_f^{0.2}$, and column 6 gives the corresponding conjugate times $t_c^{0.2}$. Note that a conjugate time marked ∞ means that no conjugate times were found within 100 times the transfer time. Columns 4 and 7 give the differences between the TCO rendezvous time and the transfer times. Note that a negative value in these columns means the transfer would be impractical, since we'd have to start the transfer before the TCO was captured (and therefore, likely before it was detected).

transfers and have to be improved. First, to refine our model the eccentricity of the orbit of the Moon around the Earth should be taken into account. This can be done for instance by using the so-called elliptic restricted problem [18] whose solution curves are more likely to model TCO trajectories in the Earth-Moon system. Additionally, the variations of the inclination of the plane of motion of the Moon around the Earth have to be considered instead of considering the mean value of this inclination as it is done in the present work. Second, the initialization methodology used in this paper to make the shooting method converge, could be refined as well. Instead of using the planar two-dimensional time-minimal transfer as the reference initial guess, each transfer to a given TCO could be used as a new initial guess to compute transfers to other TCO. This would allow to increase the number of target TCO to compute optimal transfers not only in a small vicinity of the L_1 point but in extended area within the Earth-Moon system.

Acknowledgments

This work was supported by the National Science Foundation Division of Graduate Education, award #0841223 and the National Science Foundation Division of Mathematical Sciences, award #1109937.

References

1. A.A. Agrachev and A.V. Sarychev, *On abnormals extremals for Lagrange variational problem*, J. Math. Systems. Estim. Control , **1** (1998), 87–118.
2. E.L. Allgower and K. Georg, "Numerical continuation methods, an introduction", Springer, Berlin, 1990.
3. V.I. Arnold, "Mathematical methods of classical mechanics", Springer, New-York, 1989.
4. B. Bonnard, J.-B. Caillau and G. Picot, *Geometric and Numerical Techniques in Optimal Control of the Two and Three-Body Problems*, Commun. Inf. Syst., **10** (2010), 239–278.
5. B. Bonnard B, J.-B. Caillau and E. Trélat, *Geometric optimal control of elliptic Keplerian orbits,*, Discrete Cont. Dyn. Syst. Ser. B, **4** (2005), 929–956.
6. B. Bonnard, J.-B. Caillau and E. Trélat, *Second order optimality conditions in the smooth case and applications in optimal control*, ESAIM Control Optim. and Calc. Var., **13** (2007), 207–236.
7. B. Bonnard, L. Faubourg and E. Trélat, "Mécanique céleste et contrôle des véhicules spatiaux", Springer-Verlag, Berlin, 2006.
8. B. Bonnard and I. Kupka, *Théorie des singularités de l'application entrée/sortie et optimalité des trajectoires singulières dans le problème du temps minimal*, (French)[Theory of the singularities of the input/output mapping and optimality of singular trajectories in the minimal-time problem], Forum Math., **2** (1998), 111–159.
9. B. Bonnard, N. Shcherbakova and D. Sugny, *The smooth continuation method in optimal control with an application to quantum systems*, ESAIM Control Optim. and Calc. Var., **17** (2011), 267–292.
10. J.-B. Caillau, "Contribution à l'Etude du Contrôle en Temps Minimal des Transferts Orbitaux", Ph.D thesis, Toulouse University, 2000.
11. J.-B. Caillau, O. Cots and J.Gergaud, *Differential continuation for regular optimal control problems*, Optimization Methods and Software, **27** (2012), no. 2, 177–196.
12. G. Gómez, J. Llibre, R. Martinez and C. Simó, "Dynamics and mission design near libration points", World Scientific Monograph Series in Mathematics, Volumes I, II, III, IV (2001).
13. M. Granvik, J. Vaubaillon, R. Jedicke, *The population of natural Earth satellites*, Icarus, (2012), Vol. 218, 262-277.
14. M. Guerra and A. Sarychev, *Existence and Lipschitzian regularity for relaxed minimizers*, in "Mathematical Control Theory and Finance," Springer, Berlin, (2008), 231–250.
15. W.S. Koon, M.W. Lo, J.E. Marsden and S.D Ross, "Dynamical Systems, the three-body problem and space mission design", Springer, 2008.
16. G. Picot, *Shooting and numerical continuation method for computing time-minimal and energy-minimal trajectories in the Earth-Moon system using low-propulsion*, Discrete Cont. Dyn. Syst. Ser. B, **17** (2012), 245–269.
17. L. S. Pontryagin, V. G. Boltyanskii, R. V. Gamkrelidze and E. F. Mishchenko, "The Mathematical Theory of Optimal Processes", John Wiley & Sons, New York, 1962.
18. V. Szebehely, "Theory of Orbits: The Restricted Problem of Three Bodies", Academic Press, 1967.
19. E. Trélat, *Optimal control and applications to aerospace: some results and challenges*, Journal Optim. Theory Appl., **154** no.3 (2012), 713–758.